

Selective Retina Therapy Reduces Bruch's Membrane Thickness and Retinal Pigment Epithelium Pathology in Age-Related Macular Degeneration Mouse Models

Jan Tode^{1,*}, Elisabeth Richert^{1,*}, Stefan Koinzer¹, Alexa Klettner¹, Claus von der Burchard¹, Ralf Brinkmann², Ralph Lucius³, and Johann Roeder¹

¹ Christian-Albrechts-University of Kiel, University Medical Center, Department of Ophthalmology, Arnold-Heller-Str. 3, Kiel, Germany

² Institute for Biomedical Optics, University of Lübeck and Medical Laser Center Lübeck GmbH, Peter-Monnik-Weg 4, Lübeck, Germany

³ Christian-Albrechts-University of Kiel, Institute of Anatomy, Olshausenstr. 40, Kiel, Germany

Correspondence: Jan Tode, Christian-Albrechts-University of Kiel, University Medical Center, Department of Ophthalmology, Arnold-Heller-Str. 3, 24105 Kiel, Germany. e-mail: jan.tode@uksh.de

Received: 14 February 2019

Accepted: 3 September 2019

Published: 13 November 2019

Keywords: subthreshold laser therapy; selective retina therapy (SRT); drusen; RPE morphology; dry AMD

Citation: Tode J, Richert E, Koinzer S, Klettner A, von der Burchard C, Brinkmann R, Lucius R, Roeder J. Selective retina therapy reduces bruch's membrane thickness and retinal pigment epithelium pathology in age related macular degeneration mouse models. *Trans Vis Sci Tech.* 2019;8(6):11, <https://doi.org/10.1167/tvst.8.6.11>

Copyright 2019 The Authors

Purpose: To investigate the effect of selective retina therapy (SRT) on age-related macular degeneration (AMD)-like alterations of retinal pigment epithelium (RPE) and Bruch's membrane (BrM) in AMD mouse models as therapeutic approach for the treatment of dry AMD.

Methods: In B6.129P2-ApoE^{tm1Unc}/J (ApoE^{-/-}) and B6.129X1-Nfe2l2^{tm1Ywk}/J (NRF2^{-/-}), one randomized eye of each mouse in groups of 15 mice was treated by SRT (532 nm, 300 ms, ~1.4-μs pulse, 100 Hz, 50-μm spot), the fellow eye and healthy C57BL/6J mice served as controls. Clinical examinations were obtained at treatment day and 1 month later, followed by enucleation to analyze BrM thickness and ultrastructural RPE morphology.

Results: Nearly all ApoE^{-/-} and NRF2^{-/-} mice showed AMD-like retinal alterations. BrM thickness was increased in both mouse models, RPE had vacuoles within the cell body and shortened apical microvilli. SRT neither affected neuroretinal anatomy nor function. BrM thickness as well as AMD-like ultrastructural alterations of the RPE were significantly reduced in laser-treated eyes compared with fellow control and untreated control eyes.

Conclusions: SRT reduces BrM thickness and AMD-like RPE alterations in AMD mouse models without damage to structural or functional properties of neuroretina. It may be a prophylactic or therapeutic option for dry AMD.

Translational Relevance: SRT shows therapeutic effectivity in murine AMD models and might therefore become an option for the treatment of dry AMD.

Introduction

Age-related macular degeneration (AMD) is the leading cause for legal blindness of the elderly in the developed world.¹ Currently, there is no effective prophylactic or therapeutic means to address early stages of AMD and prevent disease progression to sight-threatening advanced AMD.

Early AMD is characterized by retinal pigment epithelium (RPE) alterations with pigment clumping and metabolic deposits in and around Bruch's membrane (BrM) and RPE,^{2,3} called drusen. These

signs of early AMD are present in nonexudative (dry) AMD. Dry AMD may develop to slowly progressive RPE and neuroretinal atrophy or it may evolve to fast progressive exudative (wet) AMD, characterized by the appearance of pathological neovascularization of the choroid.⁴ Both advanced forms of AMD (dry and wet) lead to legal blindness in their natural course.

Generally, four assumptions underlie the multifactorial pathology of AMD, including impairment of lipid metabolism, extracellular matrix modifications, inflammatory processes, and altered angiogenesis. This concept has been described in detail elsewhere.^{5,6}

Briefly, key features of AMD that can be judged morphologically are a pathologically thickened BrM and altered RPE ultrastructure with shortened microvilli (mv) and intracellular vacuoles and deposits.⁷ A therapeutic means to reduce BrM thickness and restructure/rejuvenate RPE could therefore be a promising option to cure early stages of AMD and prevent disease progression. To date, there is no effective treatment that addresses early AMD-related pathology.

After a period of unhelpful laser irradiation modalities, mainly leading to retinal damage instead of rejuvenation of RPE,^{8–10} new laser approaches have been evaluated in the cure of macular disease.

Retinal Rejuvenation Therapy (2RT; Ellex ophthalmic lasers, Adelaide, Australia) is a photomechanical laser therapy, already applied within the scope of a clinical trial aiming at the treatment of dry AMD.¹¹ It is a nanopulsed approach leading to selective RPE damage within large 400- μ m spots. A beneficial effect on the progression of dry AMD could not be shown generally. In a subgroup analysis of patients without reticular pseudodrusen (RPD) disease progression could be inhibited. The speckled laser spot with areas of higher and areas of lower energy within one spot, may lead to partial over- or undertreatment and has shown to induce retinal bleeding in 6.8% of the patients.¹¹

The photomechanical selective retina therapy (SRT) is a laser treatment modality that neither affects neuroretinal anatomy nor function. SRT^{12–15} uses a train of microsecond laser pulses that leads to the formation of microbubbles at the intracellular RPE melanosomes, causing a selective disruption of RPE cell membranes.^{16,17} RPE cell death is followed by migration and proliferation of the remaining RPE cells until the RPE monolayer is restored.^{12,18} SRT does not induce a thermal alteration of any retinal tissue. Laser-induced selective RPE cell death is an entirely different approach from thermal stimulation of RPE cells and surrounding tissue, like we have shown previously.⁵ Thermal stimulation of the retina (TS-R) elevates the temperature within RPE cells to approximately 45°C.⁵ This changes the expression profile of various enzymes and cell mediators leading to therapeutic benefits concerning AMD pathology; however, RPE cells stay intact and alive, they are not replaced by new RPE cells. Compared with TS-R, SRT has a much higher impact on RPE, because selectively destroyed RPE cells are replaced by new cells. It is not known, if the biochemical and anatomic processes evoked are comparable between SRT and

TS-R. Therefore, a systematic examination of biochemical, functional, and anatomic events followed by SRT, like presented here, is needed.

SRT has shown therapeutic effect on central serous chorioretinopathy and diabetic macular edema as well as other entities that lead to the formation of subretinal fluid or retinal edema in clinical pilot trials.¹⁹

Our previous in vitro data has shown that SRT influences extracellular RPE secretion of AMD-relevant enzymes, such as matrix metalloproteinases (MMP) and factors, like vascular endothelial growth factor (VEGF) and pigment epithelium derived factor (PEDF) in porcine organ cultures. Active MMP-2 and PEDF are upregulated, VEGF is downregulated.⁶ Also, we could show that RPE regenerates by migration and even mitosis. In vitro studies demonstrated that treatment of human BrM with activated MMPs leads to an enhancement of transport capacity.²⁰ We hypothesize that SRT may lead to a rejuvenation of the RPE monolayer and to a restoration of the homeostasis of MMPs and thereby to a restoration of BrM, possibly facilitating trans-BrM metabolic exchange and RPE/photoreceptor nutrition. It might therefore be a therapeutic option for dry AMD.

To test this hypothesis, we evaluated the effect of SRT on BrM thickness and RPE morphology in two AMD mouse models, where untreated fellow eyes served as controls. This study is the next step in the systematic bench-to bedside evaluation of SRT as a treatment option for dry AMD consecutive to our previous work on organ cultures.⁶

Methods

AMD Mouse Models

Two knockout mouse models were chosen to cover the four assumptions that underlie the molecular mechanisms of AMD, including impairment of lipid metabolism, remodeling of extracellular matrix, inflammatory processes, and altered angiogenesis.

Apolipoprotein E (ApoE) knockout mice have a reduced catabolism of triglycerides and low-density lipoproteins and are therefore hyperlipidemic and hyperlipoproteinemic. Lipids are known to accumulate in blood vessels and in BrM in these animals leading to an increase in BrM thickness and remodeling of its structure. This strain is known to show AMD-like alterations of the choroid/BrM/RPE complex from 2 months of age.²¹

Nuclear factor E2-related factor 2 (Nrf2) knockout mice, on the other hand, lack one of the most important transcription factors of antioxidative processes. Antioxidant response elements (ARE) and drug metabolizing enzymes (DME) are downregulated in these mice leading to an increase in cellular stress and accumulation of oxidized cell metabolism products within the RPE and in BrM. This leads to secondary RPE degeneration, inflammatory processes, BrM thickening, and in elderly mice from 12 months of age, the formation of choroidal neovascularization (CNV).²² AMD-like alterations have been described from 9 months of age.

Both knockout strains (ApoE^{-/-} and NRF2^{-/-}) were purchased from the Jackson Laboratories (Bar Harbor, ME) and housed and bred at the local university animal care unit. The homozygous genotype was confirmed by PCR from tail clips. The wild-type C57BL6/J control mice were obtained from the local animal care facility. Mice were kept on a regular 12-hours night and day cycle and fed standard murine diet and water ad libitum. All animal experiments were conducted in accordance to the EU directive 2010/63/EU for animal experiments. They were approved by the animal ethics and welfare committee (approval number: V 242-7224.121-12 [61-5/14]) located at the ministry of energy transition, agriculture, environment, and rural areas in Schleswig-Holstein according to German federal and European law. Animal experiments adhere to the ARVO Statement for the Use of Animals in Ophthalmic and Vision Research.

Animal Maintenance and Anesthesia During Experiments

All examinations and laser treatment were conducted under general anesthesia. Deep anesthesia was induced by an intraperitoneal injection of a mixture of 0.05-mg/kg body weight Fentanyl (Braun, Melsungen, Germany), 5.0-mg/kg body weight Midazolam (Hameln Pharma, Hameln, Germany), and 0.5-mg/kg bodyweight Medetomidin (CP-Pharma, Bergdorf, Germany).

The animal was then placed on a rigid examination platform and body temperature was maintained within normal limits using a heating mat. Pupils were dilated by 0.025 mg/mL Phenylephrine and 0.05 g/mL Tropicamide (UKSH Pharmacy, Kiel, Germany), and eyes were covered with a protective moisturizing gel (2% methylcellulose Methocel; OmniVision, Puchheim, Germany). After examinations, the anesthesia

was antagonized by a mixture of 1.2-mg/kg bodyweight Naloxon (Braun), 0.5-mg/kg bodyweight Flumazenil (Inresa GmbH, Freiburg, Germany), and 2.5-mg/kg bodyweight Atipamezol (Orion Pharma, Espoo, Finland). Anesthesia was uneventful in all mice. Animal wellbeing was evaluated by a standard score sheet and was uneventful in all included mice. After the final examination animals were euthanized by cervical dislocation at the day of enucleation under deep anesthesia.

Examinations

All examinations were conducted under general anesthesia. All mice were examined by funduscopy using a contact fundus camera (MICRON III; Phoenix Research Labs, Pleasanton, CA). The integrity of the retina was assessed, the number of drusen-like retinal spots (DRS) was counted, RPE atrophy evaluated, and CNV noted.

Optical coherence tomography (OCT; small animal OCT; Thorlabs, Lübeck, Germany) was applied via contact optics to evaluate the retinal structure, confirm retinal integrity after laser treatment, and to confirm CNV. After laser treatment, it was used to investigate anatomic integrity of retinal layers. Retinal layer borders were determined and marked manually by a blinded investigator. Outer nuclear layer thickness was measured in a blinded standardized manner manually, using Thorlabs OCT software. Four measurements in each eye were carried out at 400 and 600 μm temporal as well as 400 and 600 μm nasal to the optic disc, before and 1 month after SRT. Thickness mean was compared by Student's *t*-test.

Fluorescein (10% Fluorescein, 60-mg/kg bodyweight in 100 μL saline intraperitoneally; Alcon Pharma, Freiburg, Germany) angiography (FLA; MICRON III) was performed after laser treatment to evaluate vessel integrity, to detect vessel leakage, and to confirm possible CNV formation.

All examinations were repeated at the day of enucleation, thus 1 month after laser treatment.

Laser Treatment

For SRT a frequency doubled Neodym-Vanadate (Nd:VO₄) experimental laser (Carl Zeiss Meditec AG, Jena, Germany) with a wavelength of 532 nm was used. The light was coupled to an optical multimode fiber of square cross section with a 70 \times 70- μm^2 core profile. The laser light was applied via contact laser-injector (Phoenix) attached to the Micron III camera.

The pilot laser was controlled visually via Micron III live fundus imaging.

Spot size was determined by the size of the laser fiber and laser injector, fixed to $50\ \mu\text{m}^2$ and could not be changed. Duration of irradiation was fixed to 300 ms. Pulse duration was approximately $1.4\ \mu\text{s}$ at 100 Hz, creating 30 pulses per spot. Similar to our previous work,⁵ the intended RPE-selective effect was titrated visually by decreasing energy at the peripheral retina from a clearly visible white burn at higher energy to a barely visible spot at lower energy. The barely but instantly visible spot was classified as threshold of definite RPE destruction with visible neuroretinal involvement. Energy was reduced by 70% to ensure RPE-selective laser damage. These invisible $50\text{-}\mu\text{m}$ laser spots were distributed uniformly across the retina at 1 spot interspot spacing to an optic disc centered approximately 50° field of view. No laser spot was aimed on vasculature nor the optic disc.

Electroretinogram (ERG)

Exemplary, murine, single, flash-focal ERG was performed in four mice just before and 1 week after laser treatment to examine safety of SRT concerning functional integrity of the retina. In general anesthesia (as described above), contact ERG (Phoenix Research Labs) was connected to the dark adapted (12 hours of darkness overnight) mydriatic mouse. Each flash had a size of 1.5 mm in diameter and a duration of 6 ms. The red-light aiming beam was centered at the optic nerve head under red-light fundusoscopic control. ERG was recorded at four increasing flash intensities of 2, 3.2, 4.4, and $5.6\ \text{cd}/\text{m}^2$, resulting in -0.9 , 0.3 , 1.5 , and $2.7\ \log\ \text{cd}/\text{m}^2$. For the first intensity 10 sweeps were conducted at 0.7 second delay each. All other intensities were repeated six times, the second intensity at 20 seconds delay each flash, the third at 60 seconds delay, and the fourth at 90 seconds delay between each flash. The amplitude of ERG graphs was evaluated, merged, and compared intraindividually. Means of A- and B-wave amplitudes pre- and postlaser were compared by Student's *t*-test. All other clinical examinations were carried out after ERG to avoid light confounder.

Transmission Electron Microscopy (TEM)

As described elsewhere⁵ posterior cups of enucleated murine eyes were fixated and araldite embedded for TEM. Samples were cut by microtome to sections of 100 nm following a standardized protocol. The first

set of three sections was conducted inferior to the rim of the optic nerve, the second set crossed the optic nerve and the third set of sections was superior to the rim of the optic nerve.⁵ These sections were contrasted and then examined by TEM Zeiss EM 900. To eliminate observer bias, the calculation of BrM thickness was done in a standardized and blinded manner by a single scientist. One picture at 3000-fold magnification and three pictures at defined spots in proximity to grid bars anterior to the optic nerve and three pictures posterior to the optic nerve at 12000-fold magnification were taken. The first picture was always taken strictly behind the first grid bar adjacent to the start of regular RPE morphology in proximity to the optic nerve cavity (where there is no RPE). The second picture was taken strictly before the second grid bar and the third picture strictly behind the second grid bar. The picture at lower magnification was taken to evaluate RPE morphology. Three measurements at defined spots within each picture were conducted to determine RPE's length of apical mv. Vacuole-like cytoplasm alterations were counted throughout the picture. At higher magnification, three measurements per picture were carried out to determine BrM thickness, making up a total of 54 measurements per eye. Areas of intercapillary pillars were left out.⁵

Scanning Electron Microscopy (SEM)

Because SRT spots are invisible in mice if examined by clinical methods, a top view method of the RPE monolayer is needed to visualize the effect. TEM images can only show individual cell morphology, therefore, SEM was chosen to provide an overview of treated murine retina. Two eyes of two BL/6J mice were treated by SRT exemplary. One eye was lasered by SRT with decreasing energy levels in a row fashion and correlated to clinical findings. The other eye was lasered by SRT with four suprathreshold marker lesions in a square-like orientation, a treatment energy (30% of clinical visibility) laser spot was applied in the middle of the marker spots to enable localization. Approximately 5 hours after laser treatment, these eyes were enucleated, the anterior segment and neuroretina were surgically removed and the posterior cup was fixed in 2.5% glutaraldehyde for the night. The tissue was rinsed in 0.1 M phosphate buffer and treated with 2% osmium the next day. Following dehydration by increasing ethanol concentrations, the explants were dried by a critical point dryer and sputtered with gold targets. Samples were

then investigated using a XL20 SEM (Philips, Eindhoven, Netherlands).

Genotyping

The validity and homogeneity of the intended genotype as well as screening for retinal degeneration 8 mutation of Crumbs-homologue 1 (CRB1^{rd8}), known to confound retinal phenotype, was determined by PCR from tail clips. According to Mehalow et al.,²³ for CRB1^{rd8} the following set of primers was used: mCRB1 mF2 (5'-GCCCTGTTTGCATGGAGGAAACTTGGAAGACAGCTACAGTTCTTCTG-3'), mCRB1 mF1 (5'-GTGAA-GACAGCTACAGTTCTGATC-3') and mCRB1 mR (5'-GCCCATTTGCACACTGATGAC-3'). NRF2 mice were genotyped because breeding was more productive in homozygous NRF2^{-/-} + heterozygous NRF2/+ mice, but only homozygous NRF2^{-/-} could be included into the study. According to manufacturer's specifications, for NRF2 the following primers were used: NRF2 c_forward (5'-GCCTGAGAGCTGTAGGCC-3'), NRF2 Wt_reverse (5'-GGAATGGAAAATAGCTCCTGCC-3'), and NRF2 Mut_reverse (5'-GACAGTATCGGCCTCAGGAA-3'). ApoE mice were not genotyped before experiments, because all parental mice were homozygous as specified by the vendor.

After PCR an agarose gel electrophoresis was carried out. Because two makeups were prepared, for CRB1^{rd8} two possible genotypes were expected, including wild type (220 base pairs) and mutant (244 base pairs). For NRF2 one makeup was prepared, hence three possible genotypes were expected, including wild type (262 base pairs), heterozygous (262 and 400 base pairs), and homozygous (400 base pairs).

Experimental Protocol

First, the validity of the two knockout strains as representative of AMD was to be confirmed. Untreated C57BL/6J mice of 5, 9, and 13 months of age were examined clinically (funduscopy, OCT, FLA) and by TEM. ApoE^{-/-} of 9 and NRF2^{-/-} of 13 months of age were also examined as untreated control. For the untreated controls both eyes were included. Then, experimental treatment groups had to be defined. From the literature it is known that most ApoE^{-/-} mice at the age of 8 months as well as most NRF2^{-/-} mice at the age of 12 months show AMD-like alterations of the choroid/BrM/RPE complex.^{21,22} We have confirmed AMD-like alterations in both models at that age before.⁵ ApoE^{-/-} mice were included and treated at

the age of 8 months, NRF2^{-/-} mice at the age of 12 months. Because the treated mice were enucleated 1 month after SRT, at the age of 9 months for ApoE^{-/-} and 13 months for NRF2^{-/-}, untreated controls were also chosen at comparable ages.

One randomized eye of each mouse in the two different treatment groups of 15 mice each was treated by SRT, the fellow eye served as control (see Table 1).

Statistics and Power Calculation

The primary endpoint of the study was BrM thickness. Secondary endpoints were alterations of the AMD-like phenotype (number of DRS), ultrastructural changes of the RPE (length of RPE's apical mv and number of vacuole-like cytoplasm alterations/inclusion bodies), and safety analysis of the treatment (ERG for functional analysis and OCT for anatomic analysis, see Methods sections Examinations and ERG). Comparison of laser effect was done intra-individually. Assuming Cohen's large effect size of 0.8, a type I error of 0.05 and type II error of 0.2 a group size of 15 mice each would be needed to generate a power of 0.8 (G*Power 3.1.6; Heinrich-Heine-University, Düsseldorf, Germany). Control groups were reduced to three mice each, because both eyes could be included into the determination of BrM thickness. BrM thickness was determined as the mean of 54 measurements per eye. Values were compared by paired and unpaired two-sided *t*-test, a confidence interval of 95% was chosen, *P* values ≤ 0.05 were considered significant. Statistics were calculated by R (www.r-project.org).

Results

Description of the AMD Mouse Model

Clinical examinations were carried out to determine the AMD like phenotype of the two strains. Fundus images revealed that nearly all ApoE^{-/-} and NRF2^{-/-} mice had AMD-associated retinal alterations like DRS (see Table 2) and areas of hypopigmented RPE (see Fig. 1). OCT showed various changes in the choroid/BrM/RPE/neuroretina architecture in the vicinity of DRS and hypopigmentations, associated with an AMD phenotype. Prominent DRS were seen adjacent to the RPE, mostly deforming the structure of the neuroretina (see Fig. 1). Funduscopically identified larger areas of multiple DRS mostly appeared as gap-like alterations in the pigmented choroid layer. Clinically presumed CNV

Table 1. Animal Study Groups

Strain	Age, mo	Control (c), Laser (L)	<i>n</i> , Mice	<i>n</i> , Eyes	<i>n</i> , Measure
BL/6J	5	c untreated	3	6	324
BL/6J	9	c untreated	3	6	324
BL/6J	13	c untreated	3	6	324
ApoE ^{-/-}	9	c untreated	3	6	324
NRF2 ^{-/-}	13	c untreated	3	6	324
ApoE ^{-/-}	9	c treated	15	15	810
ApoE ^{-/-}	9	L treated	15	15	810
NRF2 ^{-/-}	13	c treated	15	15	810
NRF2 ^{-/-}	13	L treated	15	15	810

Number of mice, eyes and measurements included in each group. Above: untreated controls, both eyes were included. Below: laser treatment groups, untreated fellow eyes were controls.

could well be detected by OCT and was only seen in three NRF2^{-/-} eyes. This was confirmed by FLA.

AMD-like alterations differed depending on the mouse strain. They were more severe and diverse in NRF2^{-/-} than in ApoE^{-/-} mice. These alterations were never seen in BL/6J wild-type mice. All NRF2^{-/-} mice were homozygous NRF2 knockout and homozygous CRB1^{rd8}. ApoE^{-/-} and BL/6J wild-type mice were CRB1^{rd8} negative.

Anatomic and Functional Safety of SRT

Apart from the question of the influence of SRT on BrM thickness and fundus phenotype, further focus was put on safety. To assess safety, fundus, OCT, and FLA images were compared before and 1 month after SRT and no structural changes were seen. All retinal layers remained unaltered. Clinically, no laser-induced spots with changes in fundus pigmentation were noted. FLA did not reveal any leakage. OCT showed intact neuroretinal layers. Thickness of the outer nuclear layer (ONL), measured by OCT in a standardized blinded manner, before SRT (ApoE^{-/-}: mean 57.35 μm, SEM 1.0, *n* = 5 eyes, 20 measurements; NRF2^{-/-}: mean 59.2 μm, SEM 0.98, *n* = 5 eyes, 20 measurements) compared with 1 month after SRT (ApoE^{-/-}: mean 57.4 μm, SEM 0.7, *n* = 5 eyes, 20 measurements; NRF2^{-/-}: mean 59.15 μm, SEM

0.85, *n* = 5 eyes, 20 measurements) in the same eyes of the same individuals, was unchanged (ApoE^{-/-} *P* = 0.97; NRF2^{-/-} *P* = 0.96).

In an exemplary experiment, one murine eye was lasered by SRT in a row-like pattern with decreasing energies to correlate clinical findings with SEM imaging (see Figs. 2A, 2B). Clinically, titration lesions could clearly be demonstrated by funduscopy, by OCT (also indicating damage to the neuroretina) and to a lesser degree by FLA (Fig. 2B). These spots could well be shown by SEM (Fig. 2A). Treatment spots (mean 2.4 μJ ± 1 SD), at 30% energy level of threshold (7.9 μJ ± 1.4 SD), were clinically invisible shortly after SRT, proving to be unharmed to the neuroretina. SEM revealed that treatment spots (see Figs. 2C middle circle and 2D) led to mild, but visible RPE damage. The configuration of surrounding RPE cells reminded of regeneration by migration as has been shown in organ cultures.⁶

Functionally, no significant differences in ERG amplitudes of a- and b-waves at all stimulation parameters were seen between eyes before SRT and 1 week after SRT treatment (see Fig. 3 and Table 3). The recorded ERG proved safety of SRT with respect to neuroretinal function. This measurement was carried out exemplary in four murine eyes, the ERG signals were merged (see Fig. 3).

Table 2. Number of DRS

Strain	<i>n</i> of DRS, ctrl pre	<i>n</i> of DRS, ctrl post	<i>n</i> of DRS, SRT pre	<i>n</i> of DRS, SRT post
ApoE ^{-/-}	2 (min 0; max 5)	2 (min 0; max 5)	2 (min 0; max 31)	2 (min 0; max 30)
NRF2 ^{-/-}	36 (min 1; max 210)	35 (min 1; max 202)	20 (min 1; max 215)	21 (min 1; max 200)

Median number of drusen-like retinal spots (DRS). The NRF2^{-/-} phenotype had more DRS than the ApoE^{-/-} mice. There were no differences before and after SRT concerning the number of DRS in both strains. CNV was only noted in 3 eyes of 3 NRF2^{-/-} mice.

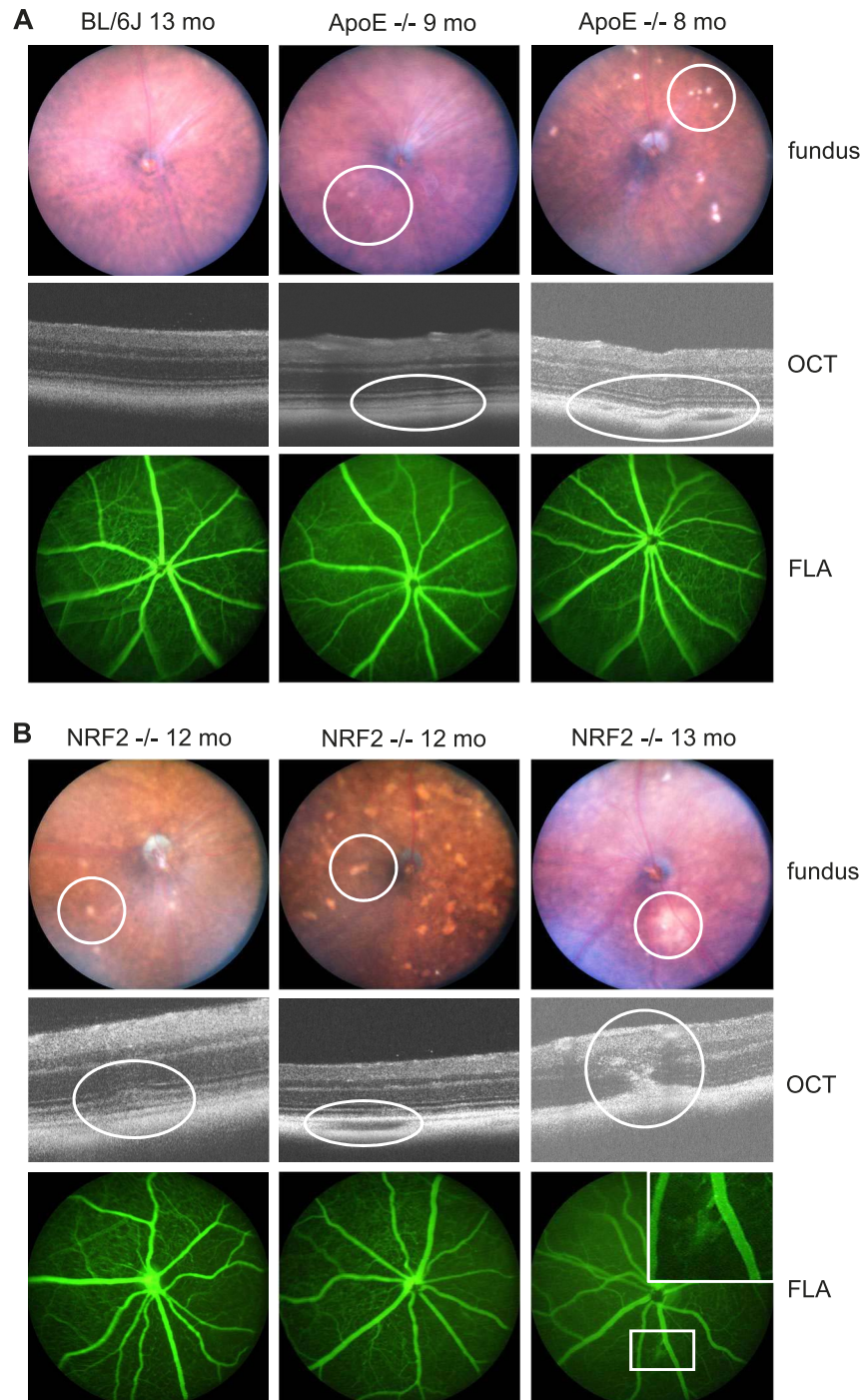


Figure 1. Phenotype. (A) depicts a wild-type 13-month-old BL/6J mouse (*left column*) showing no AMD-like fundus alterations neither funduscopically (*above*), nor by OCT (*middle*), nor by FLA (*below*). Eight months (pre-SRT), as well as 9-month-old (1 month post SRT) ApoE^{-/-} mainly showed mild AMD-like alterations (*middle column*) and rarely a phenotype of increased AMD-like alterations (*right column*). At the day of enucleation, 1 month after SRT, hence 9-month-old animals, there were no visible laser-induced alterations. DRS, as shown in the *right column*, funduscopically looked like drusen. OCT revealed, though, that they were mostly an area of hypopigmented, gap-like choroid adjacent to BrM. (B) Twelve-month-old (pre SRT), as well as 13-month-old (1 month post SRT) NRF2^{-/-} mice showed a more severe AMD-like phenotype than ApoE^{-/-}. Prominent DRS (*left column*), hypopigmented DRS-/atrophy-like areas (*middle column*) and in three eyes CNV formation connected to multiple DRS (*right column*) were typical for the NRF2^{-/-} phenotype. In FLA images, CNV could be confirmed, if present. However, neither DRS nor possibly laser-induced hyperfluorescent spots were visible in FLA images.

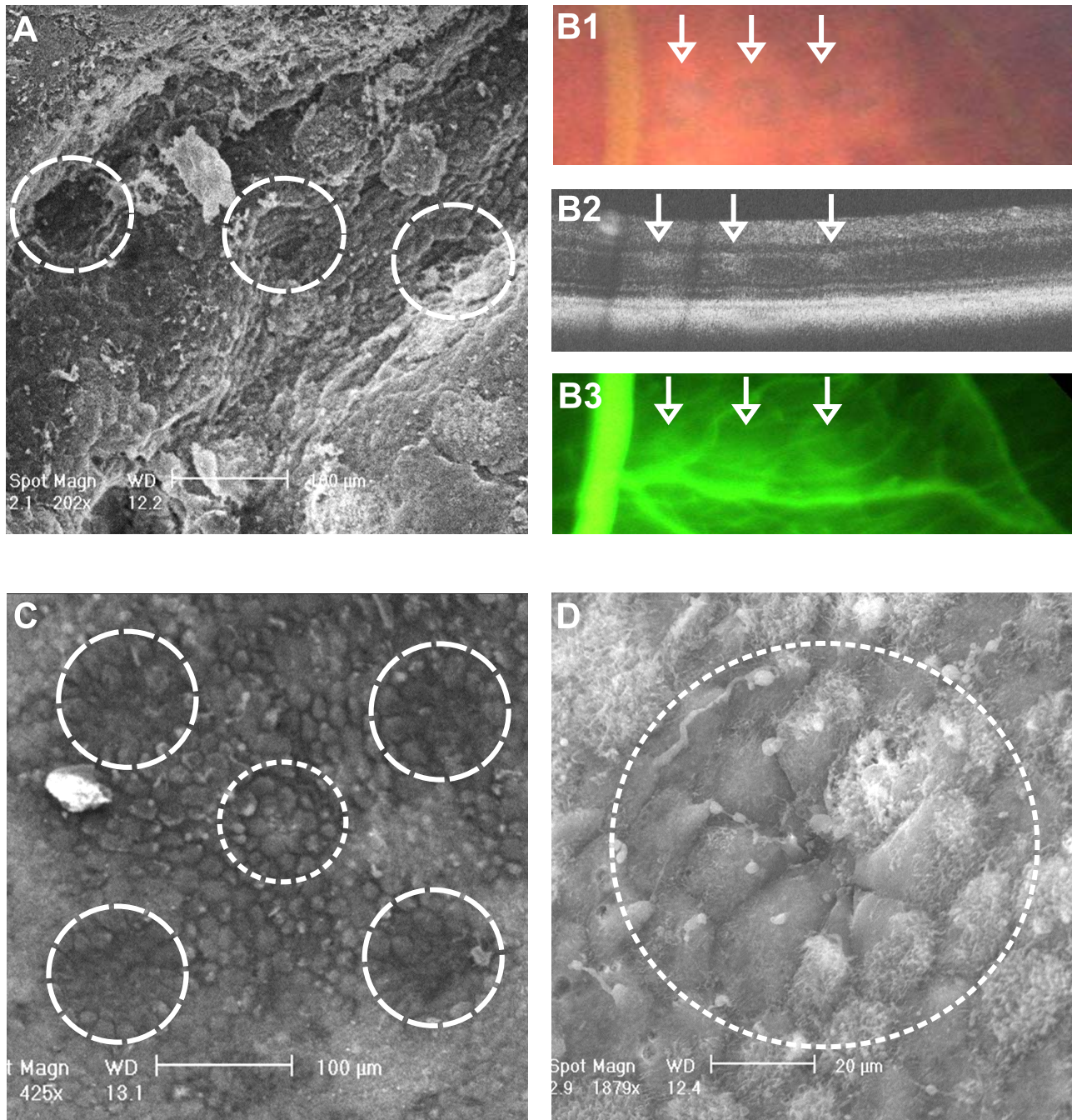


Figure 2. Structural SRT Effect. (A) SEM image of murine retina after SRT-titration in a row-pattern with decreasing energy levels (10, 8.5, 7 [threshold] μJ). The neuroretina and retinal vessels were removed before fixation. (B1) fundus image of the same titration spots, (B2) OCT, and (B3) FLA. Note how little FLA leakage is found. Treatment spots could not be displayed by in vivo imaging. (C) SEM image of a treatment spot (*middle circle*, 2.5 μJ) surrounded by suprathreshold marker lesions (*other circles*, 12 μJ). (D) Magnification of the treatment SRT spot. Note the configuration of the spot-surrounding RPE cells. There is a gap in the RPE layer revealing the underlying BrM in the middle of the spot. The surrounding cells look like migrating cells on their way to close the gap 5 hours after SRT.

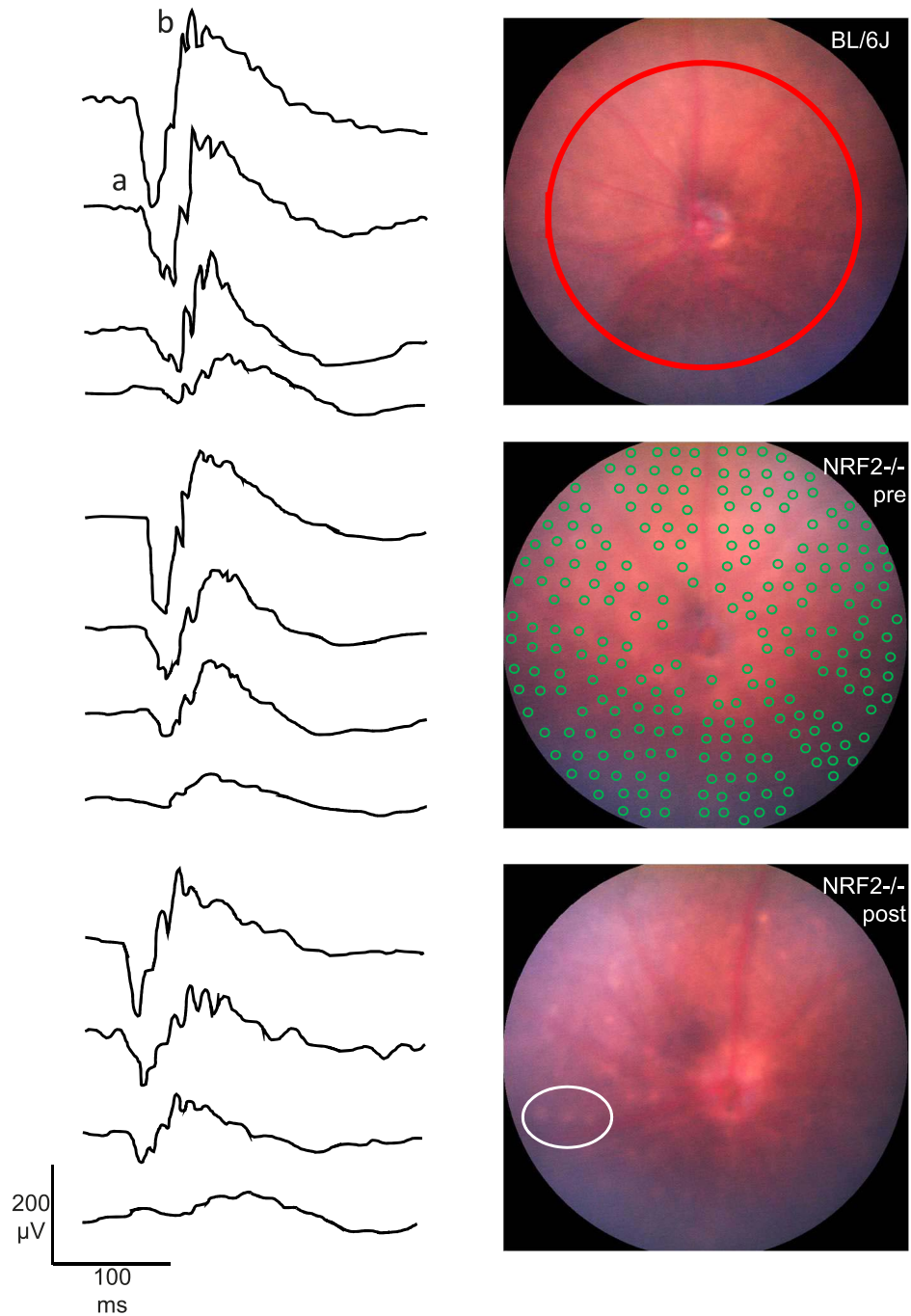


Figure 3. Safety, ERG. Merged ERG recordings of four age-matched 12-month-old BL/6J eyes (*upper row*), including one representative fundus image and four NRF2^{-/-} eyes just before SRT (*middle row*, the *green circles* schematically show the laser treatment regime applied to a representative fundus) and 1 week after SRT (*lower row*). The dark-adapted ERG was recorded at four light intensities in single-flash (6 ms) mode. Flash intensities from bottom to top -0.9 , 0.3 , 1.5 , and 2.7 log cd/m⁻². There was no statistically significant difference (P values > 0.05 ; t -test; for detailed analysis see [Table 3](#)) in mean A- and B-wave amplitude before and 1 week after SRT, proving an intact retinal function. Funduscopically, merely visible mild laser spots (*encircled*) were seen 1 week after SRT. Laser spots were never seen 1 month after SRT.

Table 3. ERG Amplitudes Pre- Versus Post-SRT

Flash, log cd s m ⁻²	Pre-SRT	Post-SRT	<i>P</i>	Pre-SRT	Post-SRT	<i>P</i>
	A-Wave Amp., Mean (SEM), μV	A-Wave Amp., Mean (SEM), μV		B-Wave Amp., Mean (SEM), μV	B-Wave Amp., Mean (SEM), μV	
-0.9	-17.0 (3.4)	-8.9 (4.2)	0.09	48 (9.5)	30 (3.7)	0.09
0.3	-52.4 (20.3)	-40.3 (23.3)	0.76	144.2 (29.1)	73 (13.5)	0.12
1.5	-116.2 (31.4)	-115.8 (28.2)	0.99	191.5 (44.7)	223.8 (45.7)	0.54
2.7	-161.1 (40.5)	-182.2 (35.9)	0.7	296.3 (46.7)	265.1 (45.3)	0.57

Mean A-wave and B-wave amplitudes ($n = 4$, each) at given flash intensities in focal ERG as shown in Figure 3, SEM. These eyes are measured before and 1 week after SRT. There were no significant differences (P values given, t -test) between the amplitudes of A- and B-waves before and after SRT.

Ultrastructural and Morphologic Description of the Model and Effect of SRT

In TEM images RPE and BrM of both ApoE^{-/-} and NRF2^{-/-} AMD mice were altered ultrastructurally in a model-specific way compared with aged wild-type BL/6J mice (see Figs. 4, 5). ApoE^{-/-} mice had a reduced length of apical mv, an increased number of vacuole-like cell plasma changes and an increased BrM thickness with multiple intra-BrM deposits (see Figs. 4–7). NRF2^{-/-} RPE was much more altered in structure than ApoE^{-/-}. There were more vacuole-like cell plasma changes. Cell bodies often appeared deformed. Apical mv were also shortened and BrM thickness was increased (see Figs. 4–7).

Primary Endpoint Bruch's Membrane Thickness

To determine the effect of SRT on AMD in our mouse models, BrM thickness was measured as primary endpoint (see Fig. 6).

In treatment naïve ApoE^{-/-} (mean 579 ± SEM 10 nm), BrM thickness was increased ($P = 0.001$, t -test) compared with age-matched wild-type BL/6J mice (mean 538 ± SEM 8 nm). BrM thickness of SRT-treated eyes (mean 430 ± SEM 27 nm) was significantly ($P = 0.048$, t -test) reduced compared with their fellow control eyes (mean 469 ± SEM 30 nm). Also, BrM thickness of control eyes was significantly ($P = 0.01$, t -test) reduced compared with treatment naïve ApoE^{-/-} eyes.

BrM thickness of untreated 13-month-old NRF2^{-/-} mice (mean 634 ± SEM 15 nm) was significantly ($P = 0.04$, t -test) higher compared with age-matched wild-type BL/6J BrM thickness (mean 546 ± 9 SEM nm). BrM of SRT-treated eyes (mean 416 ± SEM 14 nm) was significantly ($P = 0.02$, t -test) reduced compared with their fellow control eyes (mean 452 ± SEM 13

nm). BrM thickness of control eyes was significantly less ($P < 0.001$, t -test) compared with untreated NRF2^{-/-} eyes.

Secondary Endpoint RPE Cell Morphology

RPE cells are known to develop certain signs of cell stress and senescence over time and this is increased in AMD. We analyzed the length of RPE's apical mv and the number of vacuole-like cytoplasm alterations (see Fig. 7). We saw a decreasing length of mv with age ($P < 0.001$, t -test) in wild-type BL/6J mice (9 months mean 2480 ± SEM 49 nm, 13 months mean 2086 ± SEM 68 nm). Length of apical mv in SRT-treated ApoE^{-/-} mice (mean 1982 ± SEM 45 nm) was significantly ($P = 0.016$, t -test) increased compared with their fellow control eyes (mean 1781 ± SEM 60 nm). In NRF2^{-/-} mice length of apical mv was also significantly ($P = 0.002$, t -test) increased in SRT-treated (mean 1947 ± SEM 51 nm) compared with fellow control eyes (mean 1711 ± SEM 48).

The analysis of vacuole-like alterations of RPE cytoplasm, possibly morphologic correlate of lipid inclusion bodies, was counted. Cell body morphology was very diverse especially in NRF2^{-/-} (see Fig. 5). The number of vacuoles was reduced ($P = 0.01$, t -test) in SRT-treated eyes (mean $n = 6 ± SEM 1.2$) compared with fellow control eyes (mean $n = 2 ± SEM 0.3$) only in ApoE^{-/-} mice. There was no difference between SRT-treated and control in NRF2^{-/-} mice. BL/6J mice rarely had these vacuoles.

Discussion

We present here that SRT significantly reduces BrM thickness, known to be pathologically enlarged in AMD in two AMD mouse models. A thickened BrM leads to impaired gas and nutrient exchange,

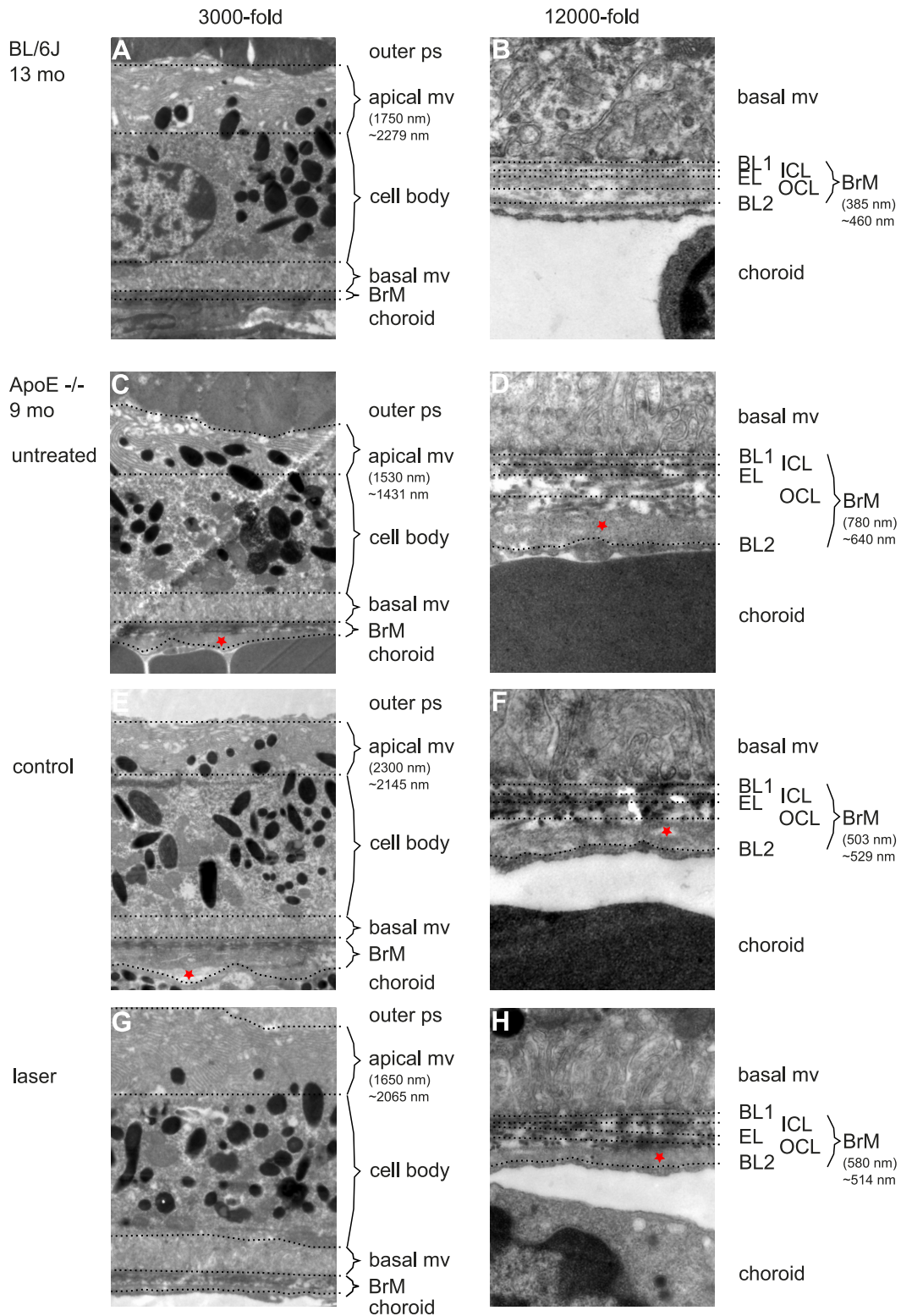


Figure 4. Secondary endpoint RPE morphology. (A) Three thousand-fold magnification of BL/6J RPE at 13 months of age. Outer photoreceptor segments (ps) are adjacent to RPE’s apical mv. Length of bracket indicates the measured length at the given point. ~ represents the mean value of the given eye. Note how variable thickness determination may be depending on the point of measurement. The cell body is characterized by a homogenous cytoplasm, the centered nucleus, mitochondria, inclusion bodies, and numerous melanosomes. Basal mv connect to BrM, which is a thin, multilayered mesh between RPE and choriocapillaris (choroid). (B) Twelve

← thousand-fold magnification of BrM of the same animal (B). Note the five layers of BrM. The basal mv of RPE connect to the first layer, RPE's basal lamina (BL1). Then three layers of collagen fibers form the mesh-like character of BrM, inner collagenous layer (ICL), elastic layer (EL), and outer collagenous layer (OCL). The basal lamina of choriocapillaris (BL2) as the fifth layer connects to the fenestrated choroidal endothelium. *Bracket* indicates the thickness measured at the given point. \sim represents the mean thickness of the given eye. (C) Untreated 9-month-old ApoE^{-/-} RPE. Note the reduced and morphologically altered apical mv and outer collagenous layer deposits (*asterisk* in [D]). (E and F) Display the control eye of a lasered mouse (*asterisk* indicates lipid-like deposits, typical for ApoE^{-/-} mice). (G and H) Display the SRT-treated eye of the same mouse. Note the difference in BrM thickness between the lasered (H) and control eye (F) as well as to the untreated eye (D).

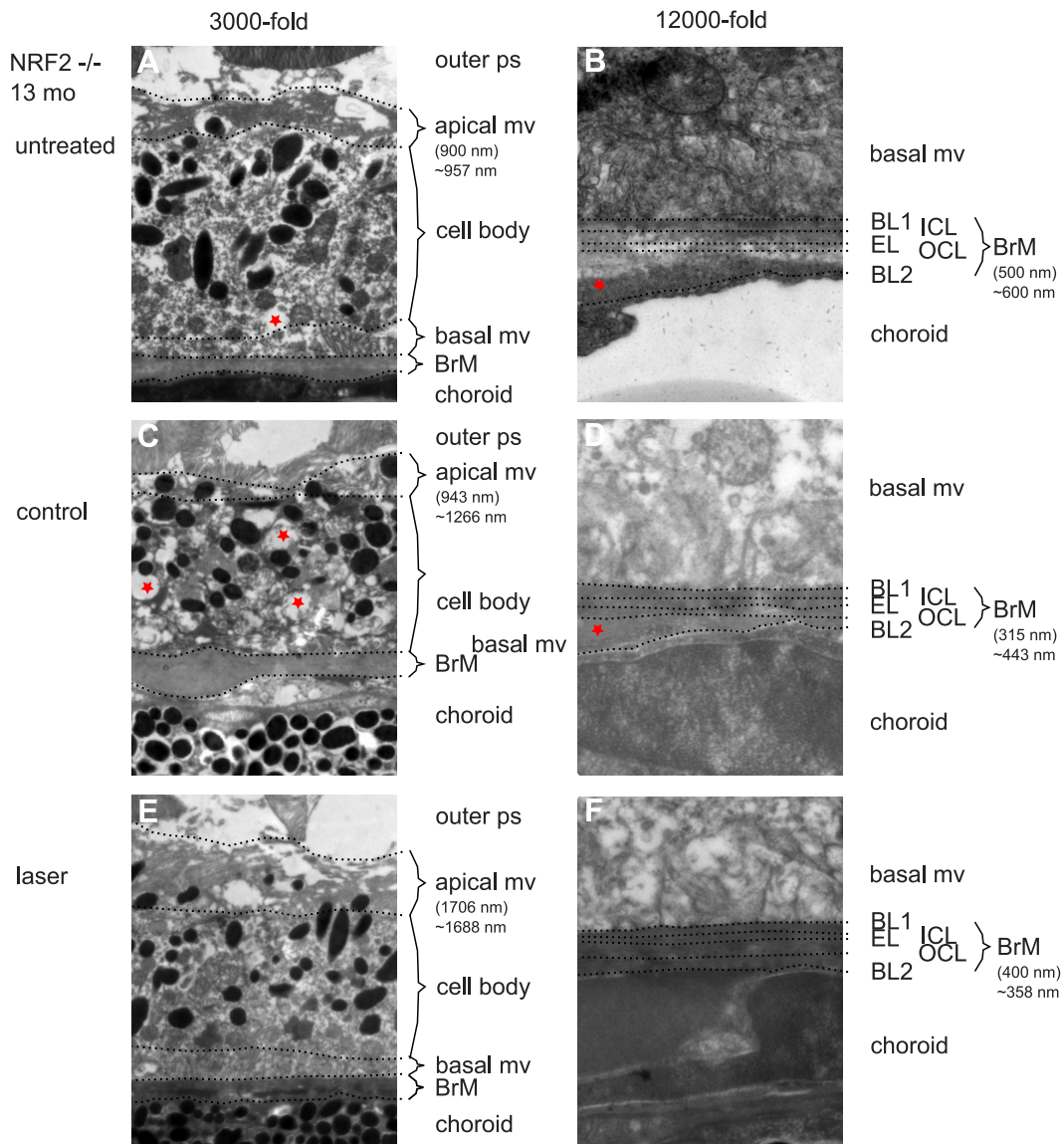


Figure 5. Secondary endpoint RPE morphology. NRF2^{-/-} mice showed a much more altered ultrastructural phenotype. Figure's presentation mode is analogous to Figure 4. Thickness measurements: *brackets* indicate the thickness measured at the given point, \sim indicates mean of the given eye. (A) untreated NRF2^{-/-} 13 months of age. Apical mv are shortened and morphologically altered/unorganized. Cytoplasm looks inhomogeneous, *asterisk* indicates a vacuole-like alteration of cytoplasm. BrM is variable in diameter and shows large outer collagenous layer deposits (B). (C) Control eyes show a similar phenotype; however, with reduced BrM thickness (D) compared with treatment naïve mice. (E) Morphologically SRT-treated RPE looks more organized and becomes similar to wild-type BL/6J RPE 1 month after treatment. (F) BrM is thinner compared with untreated mice. Thickness given in *brackets* only shows the size of the *bracket*. Measurements of BrM thickness need a standardized multimeasurements blinded system, because of variation in thickness even within one picture.

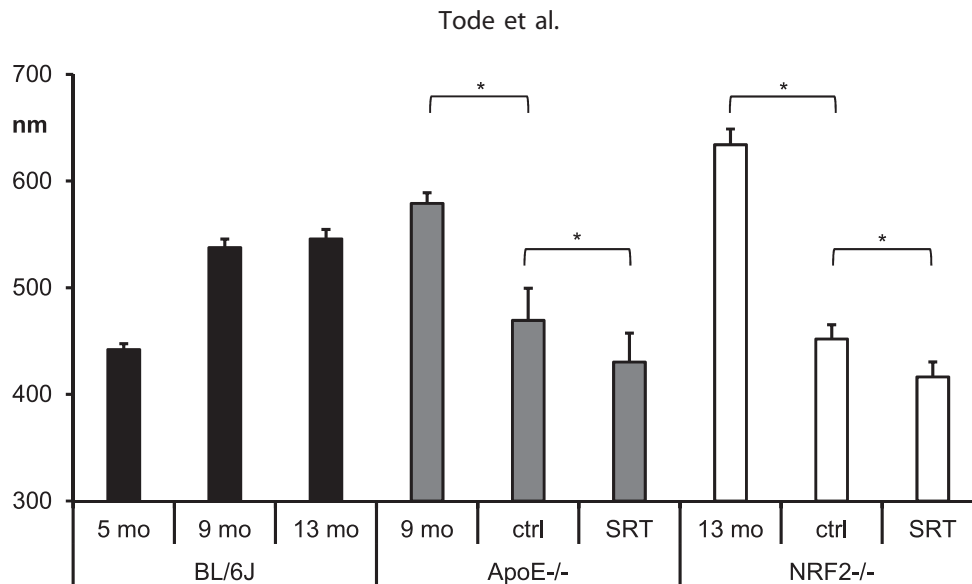


Figure 6. Primary endpoint BrM thickness. Mean BrM thickness in nano meters \pm SEM of BL/6J mice (6 eyes each) at different age (black bars), ApoE^{-/-} mice (gray bars), and NRF2^{-/-} mice (white bars). The first bar of the AMD mouse model groups shows mean BrM thickness of 6 eyes each. Control (ctrl) eyes and SRT-treated eyes are groups of 15 eyes each. The asterisks indicate statistical significance ($P \leq 0.05$) for comparison of BrM thickness between two given bars. BrM thickness of untreated eyes of both AMD models was increased compared with age matched wild-type controls. SRT-treated eyes had a decreased BrM thickness compared with their fellow control eyes. Also control eyes' BrM thickness was reduced compared with treatment naive eyes.

likely being one of the main causes for AMD. We hypothesize that a reduction of BrM thickness may facilitate gas and nutrient exchange and thereby prevent AMD disease progression or even cure the disease. Because neuroretina is left intact, SRT can even be applied to critical regions of the retina, like macula and could therefore be used as an early treatment for AMD.

Further, SRT-induced RPE cell death is known to be followed by migration and proliferation to close gaps within the monolayer.²⁴ Real proliferation is a key feature of rejuvenation. The analysis of ultra-structural changes in RPE cell morphology (Figs. 4, 4b) gives evidence for a process of revitalization or even rejuvenation with an increase in apical mv length and a reduced number of vacuoles indicating less cell stress.⁷ This reorganized and revitalized RPE (Figs. 4, 5) that follows a regenerative process after the selective deletion of RPE cells (Fig. 2), prior shown in organ cultures,⁶ suggests a positive effect toward an intact RPE monolayer with a normalized BrM mesh possibly leading to an improved photoreceptor metabolism and supply.

The clinical phenotype of our mouse models mimics AMD with DRS and pigment alterations. With ApoE^{-/-} mice reflecting the hyperlipidemic/hyperlipoproteinemic western lifestyle and with NRF2^{-/-} reflecting increased oxidative stress, two of the main driving factors of AMD are present in our

models. These two models together include all four main assumptions underlying the pathomechanism of AMD, altered lipid metabolism, changes of the extracellular matrix, inflammation, and altered angiogenesis. Our examinations allow for a statement on the effect of SRT on lipid metabolism deposits (like drusen) and extracellular matrix alterations, as well as cell morphologic changes of the RPE. Angiogenesis and inflammation were not in the focus of the study.

As shown in our previous publication,⁵ the interpretation of phenotypical AMD-like retinal alterations may be confounded by CRB1^{rd8}. It is known that this mutation mimics AMD-like pathology clinically.^{25,26} CRB1^{rd8}-linked DRS are an own entity and numerous in aged mice, even without any other genetic modification.²⁷ All NRF2^{-/-} mice included were homozygous CRB1^{rd8}, none of the other strains were affected. The variability and abundance of DRS in NRF2^{-/-} suggests CRB1^{rd8} involvement (Fig. 1). The correlate of DRS in NRF2^{-/-} CRB1^{rd8} is unclear. Gap-like lesions in the choriocapillaris (Hösel K, Tode J, Richert E, von der Burchard C, Klettner A, Roeder J. *IOVS*. 2019;60:ARVO E-Abstract 2992) or accumulation of microglial and other immune cells²⁸ are discussed correlates of DRS in CRB1^{rd8} mice. However, these DRS, enhanced by CRB1^{rd8} or not, resemble an AMD-like phenotype. Degenerative/inflammatory processes within the choroid/BrM/RPE/photorecep-

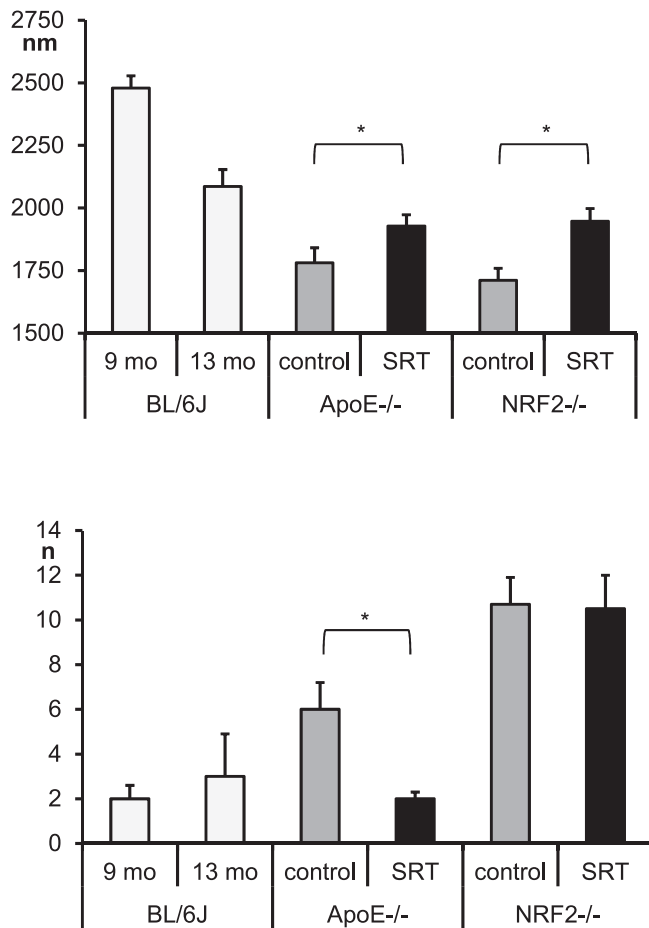


Figure 7. Secondary endpoint apical mv. *Above:* mean length of apical mv \pm SEM in nanometers. Long mv are a sign of RPE vitality. BL/6J mice (6 eyes per bar) show that mv length decreases with age. In AMD mouse models (9 eyes each ApoE^{-/-} bar, 14 eyes each NRF2^{-/-} bar), apical mv length is again reduced compared with wild type. In SRT-treated eyes, mv length increases significantly compared with the fellow control eyes. *Below:* mean number of cytoplasm vacuoles \pm SEM. A low number of vacuoles indicates healthy RPE cells. In ApoE^{-/-} the number of vacuoles is significantly reduced in SRT-treated eyes compared with their fellow control eyes. This is not the case in NRF2^{-/-}.

tor complex, possibly enhanced by CRB1^{rd8}, are typical of AMD. The study presented here is translational. The question raised here is does SRT alter the AMD phenotype, or not? It is for that reason not essential to entirely know the biochemical and molecular reasons for the AMD-like phenotype present in our murine models. It is essential to have an in vivo model that can be laser treated, with AMD-like pathology that can be measured and judged.

The pathophysiologic and biochemical properties of DRS remain unclear. In our clinical imaging modalities, funduscopically identified DRS are main-

ly a gap-like lesion in the pigmented choroid by OCT. DRS could not be imaged by FLA. To what extent immune cells are also present underneath RPE in our mouse models is unclear and should be investigated in future studies. Deposits deferring photoreceptor outer segments placed internal to the RPE monolayer (Fig. 1) were rarely seen. These deposits resemble RPD.²⁹ RPD reflect an advanced degree of AMD. Because rare in our models, an early to intermediate AMD model may be concluded.

As secondary endpoint, number of DRS were compared between SRT-treated and fellow control eyes. We did not find any significant change in number of DRS. In the absence of a good method to reliably differentiate between “real drusen” and other entities looking like drusen, this was expected. We cannot provide data on a possible effect of SRT on the number of DRS as phenotypic indicator of AMD within the scope of this study.

Safety of SRT concerning the anatomic and functional integrity of the neuroretina has been another secondary endpoint of the study. In numerous previous trials it has been proven that SRT selectively ruptures RPE cells but does neither harm structural nor functional properties of the neuroretina.^{12,14,30,31} We can show that SRT, as applied and dosed here, selectively destroys RPE cells in a controlled and spot-like manner. It does not alter the anatomic neuroretinal structure (see ONL measurements) 1 week or 1 month after laser treatment. More important, it does not have a negative effect on functional integrity. By focal ERG within the irradiated region (Fig. 3) we can demonstrate that the AMD mouse models used show reduced ERG amplitudes in both the laser-treated and the control eyes compared with age-matched wild type. However, amplitudes of the treated eyes were unaltered 1 week after SRT if compared with pre-laser ERG answers. It would be of great interest to investigate the therapeutic effect of SRT on retinal function in a large prospective animal trial.

Interestingly, after SRT BrM thickness is not only reduced in the treated, but also in the fellow control eyes, if compared with treatment naïve knockout mice in both models. This has been shown before in mice following the nanopulse laser therapy 2RT.²⁴ Thus, we support this finding rejecting the theory of it being an artefact. It is entirely unclear, how this phenomenon works. A reasonable explanation would be an autonomic regulatory process. Little is known about autonomic regulation of ocular tissues apart from the pupillary reflex arm. Certainly, there must be

numerous autonomous afferent fibers deriving from the eye's posterior segment. Concerning choroidal regulation and homeostasis, a precentral reflex arc consisting of autonomous afferents and sympathetic efferents has been proposed.³² SRT could lead to a stimulation of autonomous afferents also connecting to contralateral efferents and thereby affect the fellow untreated eye.

Also, the reduction of BrM thickness in fellow untreated eyes of SRT-treated mice raises the question, if a central treatment focus is needed, or if SRT may be applied anywhere at the fundus to reach the therapeutic goal. This question cannot be addressed in a mouse model. A differentiation between macula and periphery is impossible in murine models, because they do not have a macula region. A differentiation of therapeutic effect on BrM thickness between the treated area and peripheral retina could provide some answers and should be part of future experiments. However, to answer these questions reliably and to evaluate the needed dose (one SRT treatment or repeated SRT treatments) a prospective clinical trial in humans is imperative and will be the next step.

A reduction of BrM in fellow untreated eyes of TS-R-treated mice was not seen; however, in a smaller cohort pilot trial.⁵ This might suggest a stronger effect of SRT compared with TS-R concerning the primary endpoint. Again, it shows that RPE cell death followed by regeneration induced by SRT is different from thermal RPE stimulation evoked by TS-R.

So-called "subthreshold" laser modalities, including RPE destructive SRT and 2RT, as well as RPE stimulating TS-R and nondamaging retina therapy (NRT),³³ should not be called "subthreshold." The threshold for RPE destructive modalities is RPE cell death; a subthreshold therapy would not reach this goal and therefore be ineffective. A temperature increase is neither induced by SRT nor by 2RT. The threshold for thermal stimulatory modalities would be a certain temperature increase, likely 45°C within RPE, leaving all retinal cells undamaged. Subthreshold would account for an insufficient temperature increase and therefore be ineffective. The term "subthreshold" is broadly used, but misleading and incorrect. It derives from the idea of laser modalities that do not harm neuroretina as opposed to laser-coagulation aiming for neuroretinal damage. The above-mentioned laser modalities differ methodologically and concerning their induced effect. Each method needs to be evaluated separately. Conclusions

drawn by one modality cannot be transferred to the other, even if similarities are obvious.

Currently, there is no adequate treatment for early AMD. Dietary supplements, such as the AREDS formula, have only shown to inhibit disease progression in one eye of patients with advanced AMD in the fellow eye. As preventive measure they are controversially discussed^{34,35}

RPE-selective or thermal stimulatory laser therapies are of current interest. The first prospective double-blinded intervention compared with sham trial called "Subthreshold Nanosecond Laser Intervention in Age-Related Macular Degeneration (LEAD)" recently showed no benefit of 2RT with respect to the prevention of advanced AMD. In a post hoc analysis, though, patients without RPD had a significant benefit, patients with RPD had disadvantage of the intervention.¹¹ The study gives hope for a possible therapeutic option to address early to intermediate AMD, but more research is needed to find the correct patient group and to understand the mechanisms induced better. SRT differs from 2RT technically and with respect to its RPE selectivity. SRT laser spots are a train of microsecond pulses, 2RT is nanopulsed. SRT produces homogenous spots, the 2RT laser spots are speckled. The speckled spots might lead to overtreatment in some areas of a spot and undertreatment in other regions of the same single spot. This seems irrelevant in the peripheral retina but might be a concern in the foveal region, especially because the LEAD study showed retinal hemorrhage in 6.8% of treated patients,¹¹ suggesting damage to other tissues than RPE. So far, this complication has not been described for SRT.^{13,36}

The biochemical regenerative processes followed by either SRT or 2RT are comparable by current knowledge.

SRT is known to induce MMP secretion as latent enzymes with intracellular or membrane-associated activation preforms to fully active enzymes.^{6,37} Active enzymes can degrade all components of extracellular matrix, which stimulates cell migration and matrix turnover.^{8,39}

This could lead to a reduction of BrM thickness. SRT reduces VEGF expression and induces PEDF expression, possibly leading to an antiangiogenic milieu.⁶ The effect of SRT on inflammatory processes and on lipid metabolism must be investigated further.

Titration of the correct energy level needed to achieve a selective RPE cell death without damage to the neuroretina is still a concern. An individual automatic dosimetry that accounts for intraindividual

changes in fundus pigmentation, optical media, and alignment for every spot is important to prevent under- or overtreatment resulting in the absence of an RPE damaging or an unwanted neuroretina damaging effect, especially if aimed at the fovea region. Such a system is not available for mice and would be difficult to obtain due to the size of a murine eye. In rabbits, dosimetry systems have been established, and also in humans, dosimetry systems exist; however, not broadly available and approved.^{40–43}

The strength of this study is the large sample size of 15 animals in each of the two mouse models showing the same results with respect to the primary end point. Limitations are that not all areas of AMD pathomechanisms have been investigated. Inflammatory processes and lipid metabolism as well as the functional effect of SRT will be part of future studies. Also, dose-response investigations need to be carried out to understand the processes elicited by SRT. Laser treatment was carried out once and BrM thickness was determined 1 month after treatment. From organ culture laser experiments,⁶ we know that cell-mediator levels are altered during the first days after treatment. It is unknown whether the induction of BrM altering MMP lasts even longer. We hypothesized that a possible effect on BrM might need time to develop. We therefore chose the examination time point of 1 month after SRT. The presented data cannot give any understanding of the long-term course of disease after treatment, because we only examined at one timepoint after treatment. Mouse models have general limitations. In particular, murine eyes do not have a macula, while the anatomic structure of the retina is very similar to human retinal anatomy.

SRT is a promising and safe approach to treat dry AMD. However, seeing the sobering results of the LEAD study¹¹ pursuing a similar, yet probably entirely different approach by 2RT, and knowing that molecular understanding of the tissue response followed by SRT is limited, we will need more knowledge about the biochemical processes involved to understand how and when to use SRT to make patients benefit from the treatment and save those, who might even be at a disadvantage by the treatment. Finally, only a clinical study like the LEAD trial may help to see whether SRT might be a therapeutic option for the treatment of dry AMD or not.

Conclusion

We conclude that SRT leads to a reduction of pathologically increased BrM thickness in AMD.

Also, SRT leads to rejuvenation/revitalization of RPE. This in combination may improve photoreceptor nutrition, metabolism, and thereby function, and preserve retina from progressing to advanced AMD. SRT has the potential to be a novel and safe therapeutic and/or preventive option for early AMD.

Acknowledgments

The authors thank Serap Luick, Andrea Hethke, Katrin Neblung-Masuhr, Mandy Götz, and Frank Lichte for their excellent technical support.

Supported by the German Ministry of Education and Research (BMBF) Grant 13GW0043D.

Disclosure: **J. Tode**, None; **E. Richert**, None; **S. Koinzer**, None; **A. Klettner**, None; **C. von der Burchard**, None; **R. Brinkmann**, None; **R. Lucius**, None; **J. Roeder**, None

*Jan Tode and Elisabeth Richert contributed equally to this work.

References

1. Schrader WF. Age-related macular degeneration: a socioeconomic time bomb in our aging society [in German]. *Ophthalmol Z Dtsch Ophthalmol Ges.* 2006;103:742–748.
2. Okubo A, Rosa RH Jr, Bunce CV, et al. The relationships of age changes in retinal pigment epithelium and Bruch's membrane. *Invest Ophthalmol Vis Sci.* 1999;40:443–449.
3. Curcio CA, Johnson M, Rudolf M, Huang J-D. The oil spill in ageing Bruch membrane. *Br J Ophthalmol.* 2011;95:1638–1645.
4. CATT Research Group, Martin DF, Maguire MG, Ying GS, Grunwald JE, Fine SL, Jaffe GJ. Ranibizumab and bevacizumab for neovascular age-related macular degeneration. *N Engl J Med.* 2011;364:1897–1908.
5. Tode J, Richert E, Koinzer S., et al. Thermal stimulation of the retina reduces Bruch's membrane thickness in age related macular degeneration mouse models. *Transl Vis Sci Technol.* 2018; 7(3):2.
6. Richert E, Koinzer S, Tode J, et al. Release of different cell mediators during retinal pigment epithelium regeneration following selective retina therapy. *Invest Ophthalmol Vis Sci.* 2018;59:1323–1331.

7. Katz ML, Robison WG. Age-related changes in the retinal pigment epithelium of pigmented rats. *Exp Eye Res.* 1984;38:137–151.
8. Friberg TR, Brennen PM, Freeman WR, Musch DC; for the PTAMD Study Group. Prophylactic treatment of age-related macular degeneration report number 2: 810-nanometer laser to eyes with drusen: bilaterally eligible patients. *Ophthalmic Surg Lasers Imaging Off J Int Soc Imaging Eye.* 2009;40:530–538.
9. Friberg TR, Musch DC, Lim JJ, et al. Prophylactic treatment of age-related macular degeneration report number 1: 810-nanometer laser to eyes with drusen. Unilaterally eligible patients. *Ophthalmology* 2006;113:622.e1.
10. Parodi MB, Virgili G, Evans JR. Laser treatment of drusen to prevent progression to advanced age-related macular degeneration. *Cochrane Database Syst Rev.* 2009; CD006537.
11. Guymer RH, Wu Z, Hodgson LAB, et al. Subthreshold nanosecond laser intervention in age-related macular degeneration: the LEAD randomized controlled clinical trial. *Ophthalmology* 2019;126:829–838.
12. Brinkmann R, Roider J, Birngruber R. Selective retina therapy (SRT): a review on methods, techniques, preclinical and first clinical results. *Bull Société Belge Ophtalmol.* 2006:51–69.
13. Elsner H, Pörksen E, Klatt C, et al. Selective retina therapy in patients with central serous chorioretinopathy. *Graefes Arch Clin Exp Ophthalmol.* 2006;244:1638–1645.
14. Roider J, Liew SH, Klatt C, et al. Selective retina therapy (SRT) for clinically significant diabetic macular edema. *Graefes Arch Clin Exp Ophthalmol.* 2010;248:1263–1272.
15. Roider J, Michaud NA, Flotte TJ, Birngruber R. Response of the retinal pigment epithelium to selective photocoagulation. *Arch Ophthalmol.* 1992;110:1786–1792.
16. Brinkmann R, Hüttmann G, Rögner J, Roider J, Birngruber R, Lin CP. Origin of retinal pigment epithelium cell damage by pulsed laser irradiance in the nanosecond to microsecond time regimen. *Lasers Surg Med.* 2000;27:451–464.
17. Neumann J, Brinkmann R. Boiling nucleation on melanosomes and microbeads transiently heated by nanosecond and microsecond laser pulses. *J Biomed Opt.* 2005;10:024001.
18. Richert E, Klettner AK, Koinzer SOJ, Roider J, Hillenkamp J. Release of different cell mediators during retinal pigment epithelium (RPE) wound healing after Selective Retina Therapy (SRT) for prevention of early age-related macular degeneration (AMD). *Invest Ophthalmol Vis Sci.* 2015;56:198–198.
19. Koinzer S, Elsner H, Klatt C, et al. Selective retina therapy (SRT) of chronic subfoveal fluid after surgery of rhegmatogenous retinal detachment: three case reports. *Graefes Arch Clin Exp Ophthalmol.* 2008;246:1373–1378.
20. Ahir A, Guo L, Hussain AA, Marshall J. Expression of metalloproteinases from human retinal pigment epithelial cells and their effects on the hydraulic conductivity of Bruch's membrane. *Invest Ophthalmol Vis Sci.* 2002;43:458–465.
21. Dithmar S, Curcio CA, Le NA, Brown S, Grossniklaus HE. Ultrastructural changes in Bruch's membrane of apolipoprotein E-deficient mice. *Invest Ophthalmol Vis Sci.* 2000;41:2035–2042.
22. Zhao Z, Chen Y, Wang J, et al. Age-related retinopathy in NRF2-deficient mice. *PLoS One.* 2001;6:e19456.
23. Mehalow AK, Kameya S, Smith RS, et al. CRB1 is essential for external limiting membrane integrity and photoreceptor morphogenesis in the mammalian retina. *Hum Mol Genet.* 2003;12:2179–2189.
24. Jobling AI, Guymer RH, Vessey KA, et al. Nanosecond laser therapy reverses pathologic and molecular changes in age-related macular degeneration without retinal damage. *FASEB J.* 2015;29:696–710.
25. Mattapallil MJ, Wawrousek EF, Chan CC, et al. The Rd8 mutation of the Crb1 gene is present in vendor lines of C57BL/6N mice and embryonic stem cells, and confounds ocular induced mutant phenotypes. *Invest Ophthalmol Vis Sci.* 2012;53:2921–2927.
26. Vessey KA, Greferath U, Jobling AI, et al. Ccl2/Cx3cr1 knockout mice have inner retinal dysfunction but are not an accelerated model of AMD. *Invest Ophthalmol Vis Sci.* 2012;53:7833–7846.
27. Aredo B, Zhang K, Chen X, Wang CX, Li T, Ufret-Vincenty R.L Differences in the distribution, phenotype and gene expression of subretinal microglia/macrophages in C57BL/6N (Crb1 rd8/rd8) versus C57BL6/J (Crb1 wt/wt) mice. *J Neuroinflammation.* 2015;12:6.
28. Huang H, Liu Y, Wang L, Li W. Age-related macular degeneration phenotypes are associated with increased tumor necrosis-alpha and subretinal immune cells in aged Cxcr5 knockout mice. *PLoS One.* 2017;12:e0173716.
29. Wu Z, Ayton LN, Luu CD, Baird PN, Guymer RH. Reticular pseudodrusen in intermediate age-

- related macular degeneration: prevalence, detection, clinical, environmental, and genetic associations. *Invest Ophthalmol Vis Sci.* 2016;57:1310–1316.
30. Yasui A, Yamamoto M, Hirayama K, et al. Retinal sensitivity after selective retina therapy (SRT) on patients with central serous chorioretinopathy. *Graefes Arch Clin Exp Ophthalmol.* 2017;255:243–254.
 31. Roider J, Brinkmann R, Wirbelauer C, Laqua H, Birngruber R. Retinal sparing by selective retinal pigment epithelial photocoagulation. *Arch Ophthalmol.* 1999;117:1028–1034.
 32. Schrödl F, Schweigert M, Brehmer A, Neuhuber WL. Intrinsic neurons in the duck choroid are contacted by CGRP-immunoreactive nerve fibres: evidence for a local pre-central reflex arc in the eye. *Exp Eye Res.* 2001;72:137–146.
 33. Lavinsky D, Wang J, Huie P, et al. Nondamaging retinal laser therapy: rationale and applications to the macula. *Invest Ophthalmol Vis Sci.* 2016;57:2488–2500.
 34. Age-Related Eye Disease Study Research Group. A randomized, placebo-controlled, clinical trial of high-dose supplementation with vitamins C and E and beta carotene for age-related cataract and vision loss: AREDS report no. 9. *Arch Ophthalmol.* 2001;119:1439–1452.
 35. Evans JR, Lawrenson JG. A review of the evidence for dietary interventions in preventing or slowing the progression of age-related macular degeneration. *Ophthalmic Physiol Opt.* 2014;34:390–396.
 36. Roider J, Liew SH, Klatt C, et al. Selective retina therapy (SRT) for clinically significant diabetic macular edema. *Graefes Arch Clin Exp Ophthalmol.* 2010;248:1263–1272.
 37. Treumer F, Klettner A, Baltz J, et al. Vectorial release of matrix metalloproteinases (MMPs) from porcine RPE-choroid explants following selective retina therapy (SRT): towards slowing the macular ageing process. *Exp Eye Res.* 2012;97:63–72.
 38. Sternlicht MD, Werb Z. How matrix metalloproteinases regulate cell behavior. *Annu Rev Cell Dev Biol.* 2001;17:463–516.
 39. Woessner JF. Matrix metalloproteinases and their inhibitors in connective tissue remodeling. *FASEB J.* 1991;5:2145–2154.
 40. Seifert E, Tode J, Pielen A, et al. Selective retina therapy: toward an optically controlled automatic dosing. *J Biomed Opt.* 2018;23:1–12.
 41. Schuele G, Elsner H, Framme C, Roider J, Birngruber R, Brinkmann R. Optoacoustic real-time dosimetry for selective retina treatment. *J Biomed Opt.* 2005;10:064022.
 42. Park YG, Kang S, Kim M, Yoo N, Roh YJ. Selective retina therapy with automatic real-time feedback-controlled dosimetry for chronic central serous chorioretinopathy in Korean patients. *Graefes Arch Clin Exp Ophthalmol.* 2017;255:1375–1383.
 43. Minhee K, Park Y-G, Kang S, Roh, YJ. Comparison of the tissue response of selective retina therapy with or without real-time feedback-controlled dosimetry. *Graefes Arch Clin Exp Ophthalmol.* 2018;256:1639–1651.